

Inertia Estimation of Multi-Area Power Systems Using Tie-Line Measurements and Modal Sensitivity Analysis

Achilleas I. Sfetkos , Eleftherios O. Kontis , Theofilos A. Papadopoulos , and Grigoris K. Papagiannis 

Abstract—The replacement of conventional synchronous generators with converter-interfaced renewable energy sources (RESs) reduces the overall inertia levels of modern power systems, leading to frequency stability issues. Moreover, the intermittent nature of RESs constitutes system inertia variable during the day, further complicating the frequency control procedure. Therefore, power system operators shall estimate close to real-time the overall inertia levels of their grids in order to ensure their secure and reliable operation. In this context, in this paper, a new methodology for the inertia estimation of multi-area power systems is formulated. The proposed method uses the modal sensitivity matrix to obtain a linear approximation of the relation between modal parameters and inertia constants. During the real-time operation, modal parameters are identified via system responses using the Matrix Pencil method. The identified modes and the derived sensitivity matrix are used to estimate the overall inertia of the examined power system. The effectiveness of the proposed method is validated by means of simulations performed in one-area, two-area, and three-area power system models.

Index Terms—Frequency stability, inertia estimation, modal sensitivity, mode estimation, power system dynamics.

I. INTRODUCTION

Modern power systems face new challenges and stability issues arising from the growing integration of converter interfaced distributed energy resources (DERs) [1]. According to the European Network of Transmission System Operators for Electricity (ENTSO-E), the most important stability problems are caused due to the reduction of rotational inertia [2]. Indeed, due to environmental concerns, conventional synchronous generators (SGs), driven by fossil-fuels, are gradually decommissioned from power systems and replaced by renewable energy resources (RESs) [3], that are connected to the utility grid via power electronics [4] and do not possess inherent inertia [1].

Inertia reduction affects negatively grid frequency response, resulting in high rate of change of frequency values that may lead to frequency instability and cascaded outages [5]. Additionally, the variability of RESs production constitutes system inertia levels variable during the day, thus rendering frequency control of modern power system extremely challenging [1].

Therefore, it is very important for power system operators to estimate in real-time, or close-to-real-time, the overall inertia

levels of their grids [6], [7]. In case low inertia levels are identified, system operators can activate appropriate preventive remedial actions, such as the deployment of synchronous condensers, re-dispatching of generation units, and the reduction of power imports from neighboring bidding zones, in order to ensure the reliable and secure operation of the system [8].

In this context, during the last years transmission system operators (TSOs) and researchers have developed several inertia estimation applications exploiting wide area monitoring systems (WAMSs). For instance, in [9] an inertia calculation application, taking advantage of wide area measurements, is proposed. In this approach, frequency and active power measurements, recorded at the terminals of each SG, are used to estimate the individual inertia constants, i.e., inertia constant of each SG, via the swing equation. The overall system inertia is calculated as the weighted sum of all individual constants. Nordic TSOs have implemented inertia estimation schemes based on the monitoring of the circuit breakers (CB) of the installed SGs [8]. When the CB of a specific SG is closed, it is assumed that this SG contributes to the total kinetic energy of the system and thus to the overall system inertia. Based on this information, the total inertia levels are estimated. Nevertheless, the above-mentioned approaches require extended monitoring infrastructure to provide reliable results.

In [10], the mode shape analysis is used to determine system buses representing the center of inertia (COI) [11]. Subsequently, active power and frequency responses, recorded during transient events at COI, are used to estimate the effective system inertia via a simplified form of the swing equation. Nevertheless, transient responses are prone to noise also containing oscillatory components [4]. Thus, to eliminate the impact of these factors on inertia estimates, frequency responses are approximated using the polynomial approach of [12]. However, the order of the polynomial approximation has a crucial impact on the accuracy of the estimates [13].

In [14] the mathematical relation between inertia constants and modal parameters, i.e., frequency and damping ratio of electromechanical oscillations, is derived. Initially, modal parameters of inter-area oscillations are estimated from system responses by using system identification techniques. Subsequently, the modal parameters are used to estimate inertia constants. However, the application of this method requires the exact knowledge of the rotor angles of all the installed SGs during the steady-state operation. This requirement complicates the implementation of the method, since synchronized measurements of rotor angles cannot be easily obtained.

A. I. Sfetkos, E. O. Kontis, and G. K. Papagiannis are with the Power Systems Laboratory, School of Electrical and Computer Engineering, Aristotle University of Thessaloniki, Thessaloniki, Greece, GR 54124, (e-mail: asfetkos@ece.auth.gr; ekontis@ece.auth.gr; gpapagia@ece.auth.gr).

T. A. Papadopoulos is with the Power Systems Laboratory, Dept. of Electrical and Computer Engineering, Democritus University of Thrace, Xanthi, Greece, GR 67100, (e-mail: thpad@ee.duth.gr).

To overcome these issues, in this paper a new method for the inertia estimation of multi-area power systems is developed. In particular, the modal sensitivity matrix is used as a means to derive a linear approximation between system modal parameters and inertia constants. This enables the estimation of the system inertia under new operating conditions given the corresponding modal content. In the proposed method, the modal sensitivity matrix is computed offline by the system operator. To account for different operating conditions, the modal sensitivity matrix is computed over a range of known states, i.e., a set of states with known inertia constants. During the real-time operation, dynamic responses are used to identify via the Matrix Pencil (MP) method [15] the actual modal parameters of the examined power system. Eventually, by using the modal sensitivity matrix and the identified modal parameters the corresponding system inertia level is predicted.

The rest of the paper is organized as follows: Section II provides the theoretical background, focusing on the concept of modal sensitivity analysis. In Section III the impact of inertia constants on modal parameters is investigated. The proposed method is presented in Section IV. In Section V, a thorough evaluation of the proposed method is performed using a two-area power system model. The application of the method in one-area and three-area power systems is discussed in Section VI. Finally, Section VII summarizes the main findings and concludes the paper.

II. THEORETICAL BACKGROUND

A. Fundamental Concepts

The inertia constant H of a SG is defined as [16]:

$$H = \frac{J\omega_r^2}{2S_r} \quad (1)$$

where J [kgm²] is the moment of inertia of the SG, ω_r [rad/s] is the rated mechanical angular velocity of the rotor, and S_r [VA] is the rated apparent power of the SG.

The overall inertia constant (H_{sys}) of multi-machine power systems can be defined using (2), [16],

$$H_{sys} = \frac{\sum_i^M S_{r,i} H_i}{\sum_i^M S_{r,i}}. \quad (2)$$

Here $S_{r,i}$ and H_i denote the rated apparent power and the rated inertia constant of the i -th SG, respectively. M is the total number of the installed SGs.

B. Power System Modeling

During small perturbations, power systems can be modeled as linear time-invariant systems using the state-space representation of (3). Equations in (3) are evaluated at the operating point, around which the perturbation is considered [16].

$$\begin{cases} \dot{\mathbf{x}}(t) = \mathbf{A}\mathbf{x}(t) + \mathbf{B}\mathbf{u}(t) + \mathbf{F}\mathbf{w}(t) \\ \mathbf{y}(t) = \mathbf{C}\mathbf{x}(t) + \mathbf{D}\mathbf{u}(t). \end{cases} \quad (3)$$

Here $\mathbf{x}(t) \in \mathbb{R}^n$ is the state vector, $\mathbf{u}(t) \in \mathbb{R}^r$ is the input vector, and $\mathbf{y}(t) \in \mathbb{R}^m$ is the output vector. $\mathbf{A} \in \mathbb{R}^{n \times n}$, $\mathbf{B} \in \mathbb{R}^{n \times r}$, $\mathbf{C} \in \mathbb{R}^{m \times n}$, and $\mathbf{D} \in \mathbb{R}^{m \times r}$ are the system

matrices. Vector $\mathbf{w}(t) \in \mathbb{R}^r$ and matrix $\mathbf{F} \in \mathbb{R}^{n \times r}$ simulate the effect of disturbances in the state space model.

The eigenvalues of \mathbf{A} are given by the values of the scalar parameter λ for which there exist non-trivial solutions, i.e., other than $\phi = 0$, to the following equation [16]:

$$\mathbf{A}\phi = \lambda\phi \quad (4)$$

For any eigenvalue λ_i , the column vector $\phi_i \in \mathbb{R}^{n \times 1}$ that satisfies (4) is named the right eigenvector of \mathbf{A} associated with eigenvalue λ_i . Similarly, the row vector $\psi_i \in \mathbb{R}^{1 \times n}$ which satisfies [16]:

$$\psi_i \mathbf{A} = \lambda_i \psi_i, \quad i = 1, 2, \dots, n \quad (5)$$

is the left eigenvector of \mathbf{A} , associated with eigenvalue λ_i .

C. Modal Sensitivity Analysis

Let $\Theta = [\theta_1, \dots, \theta_i, \dots, \theta_N]^T \in \mathbb{R}^{N \times 1}$ be the set of parameters of the examined system. By differentiating (4) with respect to the i -th parameter θ_i and substituting for the j -th eigenvalue, the following equation results:

$$\frac{\partial \mathbf{A}}{\partial \theta_i} \phi_j + \mathbf{A} \frac{\partial \phi_j}{\partial \theta_i} = \frac{\partial \lambda_j}{\partial \theta_i} \phi_j + \lambda_j \frac{\partial \phi_j}{\partial \theta_i} \quad (6)$$

The sensitivity of the j -th mode with respect to parameter θ_i can be derived by performing left multiplication on (6) with the corresponding left eigenvector, ψ_j , using the definition of (5) and the normalized eigenvector property $\psi_j \cdot \phi_j = 1$ [18]:

$$\frac{\partial \lambda_j}{\partial \theta_i} = \psi_j \frac{\partial \mathbf{A}}{\partial \theta_i} \phi_j \quad (7)$$

Eq. (7) can then be used to calculate the full sensitivity matrix for a subset of the system modes $\{\lambda_1, \dots, \lambda_k\}$, [18]:

$$\mathbf{S} = \begin{bmatrix} \frac{\partial \lambda_1}{\partial \theta_1} & \cdots & \frac{\partial \lambda_1}{\partial \theta_i} & \cdots & \frac{\partial \lambda_1}{\partial \theta_N} \\ \vdots & \ddots & \vdots & \ddots & \vdots \\ \frac{\partial \lambda_j}{\partial \theta_1} & \cdots & \frac{\partial \lambda_j}{\partial \theta_i} & \cdots & \frac{\partial \lambda_j}{\partial \theta_N} \\ \vdots & \ddots & \vdots & \ddots & \vdots \\ \frac{\partial \lambda_k}{\partial \theta_1} & \cdots & \frac{\partial \lambda_k}{\partial \theta_i} & \cdots & \frac{\partial \lambda_k}{\partial \theta_N} \end{bmatrix} \quad (8)$$

The variation of system modes due to a change on model parameters can be estimated via the linear approximation

$$\Delta \Lambda \approx \mathbf{S} \cdot \Delta \Theta. \quad (9)$$

Here $\Delta \Lambda = \Lambda' - \Lambda$ denotes the variation of system modes from the known state Λ (corresponding to the set of parameters Θ) to the new state Λ' associated with the modified system parameters Θ' .

If system modes Λ' are known, e.g., by applying identification techniques to system measurements, then (9) can be used to estimate $\Delta \Theta$. In the general case, (9) expresses an over-determined problem. Thus, it can be solved in a least square sense [19] as follows:

$$\Delta \Theta = (\mathbf{S}^T \mathbf{S})^{-1} \mathbf{S}^T \Delta \Lambda. \quad (10)$$

Therefore, it is clear that any updates/modifications of model parameters can be quantified by computing Θ' via (11).

$$\Theta' \approx \Theta + \Delta\Theta \quad (11)$$

The modal sensitivity concept, described above, is used to predict inertia constants by means of the modal parameters contained in measured responses. In particular, system modes Λ and the sensitivity matrix S are computed offline assuming a set of known states, i.e., states of the examined power system with known inertia constants. Λ' is identified during real-time operation by applying the MP method to system measurements. Eventually, (11) is used to determine Θ' , i.e., values of inertia constants corresponding to Λ' .

D. Mode Estimation Using the MP Technique

The MP method is based on the singular value decomposition (SVD) of Hankel matrices, constructed using system responses $y(t)$. The implementation of the MP can be summarized by the following steps [15]:

Step-1: Construct Hankel matrices H_0 and H_1 using as entries the samples of $y(t)$.

Step-2: Perform SVD of H_0 .

$$H_0 = USV^T \quad (12)$$

Here S is a diagonal matrix containing the square root of U and V eigenvalues. U and V are singular vector matrices.

Step-3: Matrices V_1 and V_2 are constructed by deleting the last and the first row of matrix V . Subsequently, matrices Y_1 and Y_2 are computed.

$$Y_1 = V_1^T V_1 \quad (13)$$

$$Y_2 = V_2^T V_2 \quad (14)$$

Step-4: Modes contained at $y(t)$ are the generalized eigenvalues of the matrix pair $\{Y_1, Y_2\}$, resulting from

$$Y_1^{-1}Y_2 - \lambda I. \quad (15)$$

The required approximation order, i.e., the order of the MP model, is defined in this paper using the iterative procedure presented in [20]. The tolerance τ for the convergence of the iterative procedure is set to 10^{-6} .

III. IMPACT OF INERTIA ON POWER SYSTEM DYNAMICS

Here, the impact of inertia levels on power system dynamics is investigated using a generic two-area power system model.

A. System Under Study

The simulations are performed using the system frequency response (SFR) model of Fig. 1. The examined system is an inter-connected two-area power system. Both Areas have the same rated power. As shown in Fig. 1, each Area is simulated using an aggregated generator unit. Nonlinearities are considered by integrating generation rate constraints (GRC) in both aggregated units. The saturation limits are $\pm 5\%$ [17]. In the examined system, RESs are controlled by power converters according to the maximum power point tracking algorithm [21]; thus, as they cannot contribute to frequency support, RESs are not explicitly modeled and their impact on frequency dynamics is only reflected to the reduced system inertia.

In Fig. 1 ΔF_n is the frequency deviation of the n -th Area during a disturbance. ΔP_{Dn} is the change of load demand at the n -th Area and ΔP_{tie} is the incremental change of the power flowing through the system tie-line. $T_{1,2}$ is the synchronising coefficient. R_n and B_n is the speed regulation droop and the frequency bias constant of the n -th Area, respectively. $T_{g,n}$ and $T_{t,n}$ are the time constants of the governor and the turbine of the n -th Area, respectively. P_n and I_n are the proportional and the internal gain of the automatic generation control of the n -th Area. D_n is the damping coefficient of the n -th Area and f_0 is the nominal frequency. Effective inertia $H_{n,e}$ of each Area is defined as discussed in [22] using (16).

$$H_{n,e} = (1 - d_n)H_n. \quad (16)$$

Here H_n corresponds to the overall inertia constant of the n -th Area when no RESs are considered. Parameter d_n denotes the percentage of the kinetic energy displaced from Area n due to the replacement of x_n number of conventional SGs by inertia-less converter interfaced RESs [22]. x_n is known to the system operator from the results of the day-ahead market. Since, x_n is known, d_n can be computed as discussed in [22].

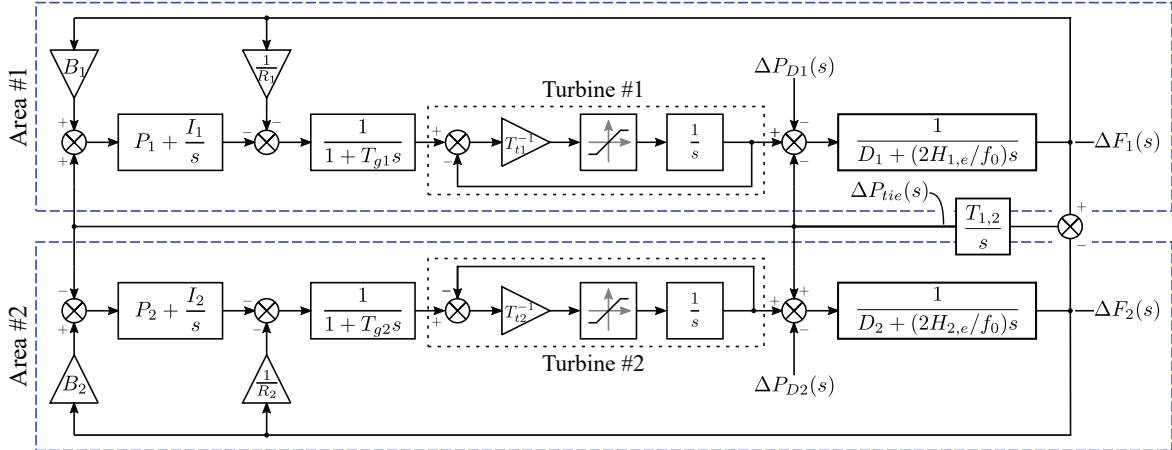


Fig. 1. SFR model of a two-area power system [17]. Values used for the simulations: $R_1 = 2.16$ Hz/MW, $R_2 = 2.64$ Hz/MW, $B_1 = 0.4675$ MW/Hz, $B_2 = 0.3825$ MW/Hz, $P_1 = 0.18$, $P_2 = 0.22$, $I_1 = 0.55$ Hz, $I_2 = 0.45$ Hz, $T_{g,1} = 0.072$ s, $T_{g,2} = 0.088$ s, $T_{t,1} = 0.33$ s, $T_{t,2} = 0.27$ s, $T_{1,2} = 0.545$ s, $D_1 = 0.0076$ pu/Hz, $D_2 = 0.0093$ pu/Hz, $H_{1,e} = 4.5$ s, $H_{2,e} = 6.5$ s, $f_0 = 50$ Hz.

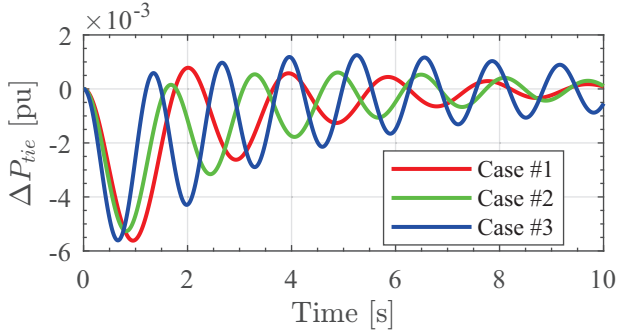


Fig. 2. Impact of low inertia levels on power system oscillations.

B. Time Domain Simulations

To quantify the impact of RES penetration on inertia levels and consequently on system dynamics, three distinct cases, namely Case#1, Case#2, and Case#3, are considered. In Case#1 the RES penetration level is equal to zero for both areas, i.e., $d_1 = d_2 = 0$ and $H_{sys} = 5.5$ s. In Case#2 the 20% of the load demand of Area#1 is covered by inertia-less converted interfaced units, i.e., $d_1 = 0.2$, and of Area#2 by 40%, thus $d_2 = 0.4$ and $H_{sys} = 3.75$ s. For Case#3, $d_1 = d_2 = 0.5$; thus $H_{sys} = 2.75$ s.

To investigate the system dynamics, the time domain response of the active power flowing through the system tie-line is used. For all examined cases a step disturbance of load demand in Area#1, $\Delta p_{D1}=1\%$ at $t=0$, is simulated. The disturbance is sufficiently small, thus the impact of GRC is not triggered. The event is simulated for 10 s, i.e., $0 \leq t \leq 10$ s. Simulations are performed assuming a time step of $T_s = 0.001$ s. To replicate realistic phasor measurement unit recordings, all responses are decimated to 100 samples per second (sps).

The impact of the reduction of inertia levels on active power oscillations is presented in Fig. 2. As shown, there is a strong relation between power oscillations and the overall inertia levels. Indeed, it is clear that as inertia levels drop, the power oscillations exhibit higher frequency and lower damping.

C. Modal Analysis

The impact of inertia levels on system dynamics is also verified by means of modal analysis. For this purpose, the detailed 9th-order state-space model of Fig. 1 is used and the corresponding eigenvalues are computed and presented in Table I. As shown, as the total inertia level is reduced, complex modes shift towards larger imaginary parts and lower real parts. Thus, resulting oscillations exhibit higher frequency and lower damping. This remark is in-line with the results presented in Fig. 2.

Instead of using eigenvalue analysis, measurement-based modal analysis can also be performed. In this case, dynamic responses of ΔP_{tie} shown in Fig. 2 are forwarded as inputs to the MP to determine modal parameters. To achieve comparable results with those presented in Table I, a 9th-order model is used for the MP. The percentage error between the actual modal parameters (computed via eigen-analysis) and those estimated using the MP method is reported in Table II. As

TABLE I
MODAL PARAMETERS COMPUTED VIA EIGEN-ANALYSIS

Mode	Case#1	Case#2	Case#3
1,2	$-0.30 \pm j3.26$	$-0.23 \pm j3.91$	$-0.13 \pm j4.82$
3,4	$-1.02 \pm j2.09$	$-0.98 \pm j2.87$	$-0.84 \pm j3.38$
5	-0.44	-0.42	-0.41
6	-0.55	-0.55	-0.54
7	-1.77	-1.52	-1.44
8	-12.06	-12.44	-12.61
9	-14.61	-14.76	-15.19

TABLE II
PERCENTAGE ERROR OF MP MODAL ESTIMATES

Mode	Case#1	Case#2	Case#3
1,2	$3.79 \cdot 10^{-7}$	$1.62 \cdot 10^{-7}$	$5.59 \cdot 10^{-8}$
3,4	$1.80 \cdot 10^{-6}$	$1.89 \cdot 10^{-7}$	$1.26 \cdot 10^{-7}$
5	$1.86 \cdot 10^{-5}$	$3.11 \cdot 10^{-6}$	$7.48 \cdot 10^{-6}$
6	$2.74 \cdot 10^{-5}$	$9.70 \cdot 10^{-6}$	$6.05 \cdot 10^{-6}$
7	$1.48 \cdot 10^{-5}$	$4.63 \cdot 10^{-6}$	$4.72 \cdot 10^{-7}$
8	$2.06 \cdot 10^{-4}$	$1.58 \cdot 10^{-4}$	$2.57 \cdot 10^{-5}$
9	$1.34 \cdot 10^{-5}$	$9.40 \cdot 10^{-6}$	$2.08 \cdot 10^{-7}$

shown, all modal parameters can be estimated very accurately by applying the MP method to system responses.

To demonstrate the accuracy of the MP method under different disturbance levels, the following analysis is performed: Inertia levels of Case#1 are considered and three disturbance levels, namely $\Delta p_{D1}=1\%$, $\Delta p_{D1}=3\%$, and $\Delta p_{D1}=5\%$, are examined. The resulting ΔP_{tie} responses are used by the MP method for mode identification. To achieve comparable results with those reported in Table I, the impact of GRC is neglected. The percentage errors against the actual modes are provided in Table III, verifying the robustness of MP.

TABLE III
PERCENTAGE ERROR OF MP MODAL ESTIMATES FOR CASE #1 UNDER DIFFERENT DISTURBANCE LEVELS

Mode	$\Delta p_{D1} = 1\%$	$\Delta p_{D1} = 3\%$	$\Delta p_{D1} = 5\%$
1,2	$3.79 \cdot 10^{-7}$	$2.54 \cdot 10^{-7}$	$2.43 \cdot 10^{-7}$
3,4	$1.80 \cdot 10^{-6}$	$2.96 \cdot 10^{-6}$	$1.30 \cdot 10^{-6}$
5	$1.86 \cdot 10^{-5}$	$6.61 \cdot 10^{-5}$	$1.05 \cdot 10^{-5}$
6	$2.74 \cdot 10^{-5}$	$7.79 \cdot 10^{-5}$	$1.39 \cdot 10^{-5}$
7	$1.48 \cdot 10^{-5}$	$2.34 \cdot 10^{-5}$	$3.68 \cdot 10^{-6}$
8	$2.06 \cdot 10^{-4}$	$1.01 \cdot 10^{-4}$	$1.58 \cdot 10^{-5}$
9	$1.34 \cdot 10^{-5}$	$3.12 \cdot 10^{-7}$	$5.63 \cdot 10^{-7}$

D. Root Locus Analysis

In this subsection, the impact of inertia levels on system modal parameters is investigated more thoroughly by means of root locus analysis. For the analysis, two discrete scenarios are considered. In the first scenario, H_2 is assumed constant and equal to 5.5 s, while H_1 varies in the interval [3 s, 8 s]. In the second scenario, H_1 is set to 5.5 s and $H_2 \in [3 \text{ s}, 8 \text{ s}]$.

Root locus analysis results for both scenarios are summarized in Fig. 3. As shown, for both scenarios as the inertia level increases, the frequency of complex modes $\lambda_{1,2}$ and $\lambda_{3,4}$ decreases monotonically. The damping of these modes

present a more complicated behavior and can either increase or decrease depending on the inertia level. Moreover, as inertia level increases, damping of mode λ_7 decreases, while damping of modes λ_8 and λ_9 increase. These results are in agreement with those presented in Table I. Finally, modes λ_5 and λ_6 exhibit different behavior depending on the examined scenario.

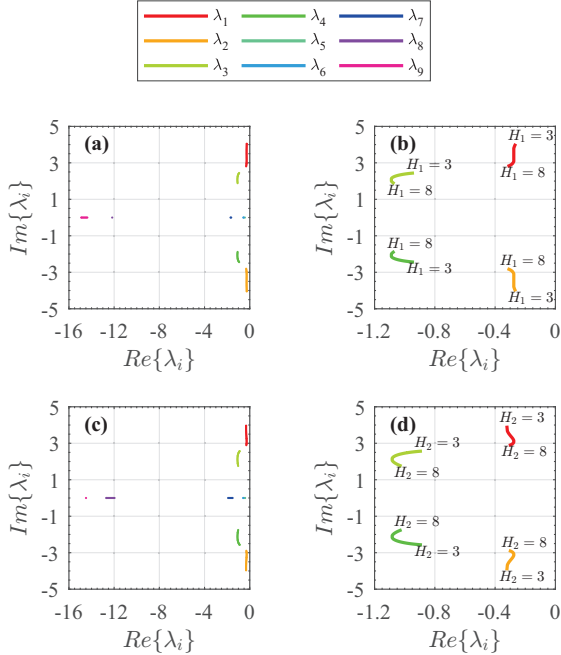


Fig. 3. Root loci for first scenario: (a) full mode set (b) complex mode set. Root loci for second scenario: (c) full mode set (d) complex mode set.

E. Discussion

The presented analysis verifies that inertia levels influence considerably the eigenvalues of the examined system and thus the frequency and the damping of the oscillations. Nevertheless, as verified by the root locus analysis, there is not a straightforward relation between inertia constants and modal parameters. Therefore, to provide a further insight, the concept of the sensitivity matrix is adopted. Additionally, the analysis reveals that measurement-based modal analysis via the MP method can provide very accurate modal estimates.

The above-mentioned remarks are used to formulate a measurement-based approach for the estimation of the overall inertia levels of inter-connected power systems. The proposed approach is analyzed in detail in Section IV.

IV. PROPOSED METHODOLOGY

The proposed methodology is presented by means of a flowchart in Fig. 4. An analysis of all steps is provided below:

Step 1: Dynamic responses $y(t)$ of the examined system, resulted from small perturbations, are recorded during the real-time operation and forwarded as inputs to the method. In case of power systems with no external interconnections, i.e., one-area systems, $y(t)$ is the time domain response of the grid frequency. In case of multi-area power systems, $y(t)$ is the time domain response of active power flowing through the

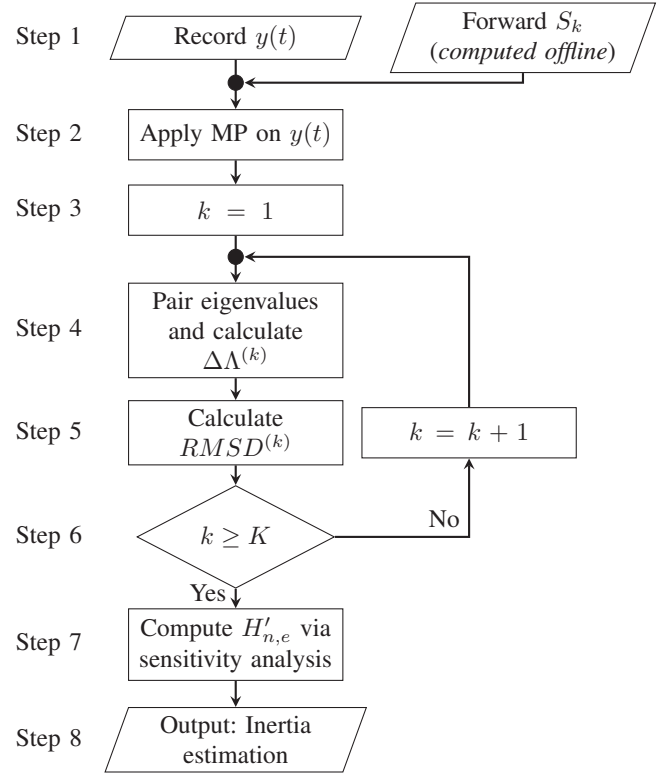


Fig. 4. Proposed method to estimate the overall power system inertia.

system tie-lines. Using only the above-mentioned responses, the number of signals, required for the implementation of the method, is minimized. Additionally, the method receives as input a total number of K modal sensitivity matrices, denoted as S_k with $k = 1, \dots, K$. Here, K is the total number of known system states. The sensitivity matrices are calculated with respect to the effective inertia $H_{n,e}$ of each area. The required calculations are performed offline by the system operator. Each sensitivity matrix corresponds to a discrete known state, i.e., to a different operating point with known parameters.

Step 2: The MP method is applied to $y(t)$ to identify modal parameters. The minimum required order for the MP method is defined using the methodology presented in [20].

Step 3: The algorithm loops through the known states, starting with the first ($k = 1$).

Step 4: The modes identified in Step 2 are paired with the modes of the k -th known state; the $\Delta\Lambda^{(k)}$ difference is also computed. For the pairing process and for the rest of the analysis only the complex (oscillatory) modes are considered. The reason is twofold: Identification of real modes under real field conditions may be problematic, due to their fast damping and thus their negligible impact on system oscillations. Additionally, as indicated by the root locus analysis of Fig. 3, complex eigenvalues are easily distinguishable. Thus, the pairing process can be simply performed by sorting complex modes by their imaginary and real parts.

Step 5: The modal parameters identified at Step 2 are compared with the corresponding modal parameters of the k -th known state. The latter are derived through the pairing process of Step 4. The comparison is performed by means of the Root

Mean Square Deviation (*RMSD*):

$$RMSD(\mathbf{\Lambda}^{(k)}, \mathbf{\Lambda}') = \sqrt{\frac{1}{M} \sum_{j=1}^M \left\| \lambda_j^{(k)} - \lambda'_j \right\|^2} \quad (17)$$

Here, $\lambda_j^{(k)}$ and λ'_j denote the j -th mode of the k -th known state and the j -th mode contained in $y(t)$, respectively.

Step 6: If more known states are available, i.e., $k < K$, then the procedure moves to Step 4. Otherwise, the procedure moves to Step 7.

Step 7: Scope of this step is to determine the unknown inertia constants $H'_{n,e}$ by using (9) - (11). Nevertheless, in order to apply (9) - (11) the modal sensitivity matrix that better describes the examined system during the real-time operation shall be identified. For this purpose, the sensitivity matrix corresponding to the k -th known state that results in the lowest *RMSD* is selected.

Step 8: The overall system inertia is calculated using (2).

V. EVALUATION OF THE PROPOSED METHODOLOGY

In this Section the impact of several factors on the performance of the proposed methodology is assessed.

A. Impact of Linearization

Eq. (9) is a linear approximation of the actual relation between system eigenvalues and model parameters, e.g., inertia constants. Therefore, the error introduced due to the linearization shall be quantified. For this purpose, the following analysis is performed: It is assumed that only one state of the examined system is known, i.e., $K=1$, with $[H_{1,e}, H_{2,e}] = [4.5 \text{ s}, 6.5 \text{ s}]$. All other model parameters are those summarized in Fig. 1. A total number of 40 unknown cases is created by varying either $H_{1,e}$ or $H_{2,e}$. In particular, twenty unknown cases are generated by varying only $H_{1,e}$ by $\pm 1\%$, $\pm 2\%$, \dots , $\pm 10\%$. Twenty additional unknown cases are generated by varying only $H_{2,e}$ by $\pm 1\%$, $\pm 2\%$, \dots , $\pm 10\%$. For all cases, the method of Fig. 4 is applied to identify H'_{sys} .

Three scenarios concerning identification of eigenvalues $\Delta\mathbf{\Lambda}'$ are considered, namely S1, S2, and S3. In S1, $\Delta\mathbf{\Lambda}'$ is defined via eigen-analysis and all modes are used to estimate H'_{sys} . In S2, $\Delta\mathbf{\Lambda}'$ is defined via eigen-analysis, but only complex (oscillatory) modes are used to estimate the unknown inertia constants. In S3, $\Delta\mathbf{\Lambda}'$ is estimated via the MP method using ΔP_{tie} dynamic responses. In all cases, the algorithm of [20] defines that a sixth order model shall be used by the MP method to accurately capture system dynamics.

Fig. 5 summarizes for all cases the absolute percentage error (*PE*) of the overall system inertia H'_{sys} , defined as:

$$|PE(\%)| = \left| \frac{H_{actual} - H_{est}}{H_{actual}} \right| \cdot 100\% \quad (18)$$

where H_{actual} is the actual inertia constant and H_{est} is the estimation provided by the proposed method. The presented results reveal that for small variations of individual inertia constants, e.g., $\pm 5\%$, the proposed method provides accurate estimates for H'_{sys} , i.e., estimates resulting in $PE \leq 5\%$. For higher variations of individual inertia constants, non-negligible

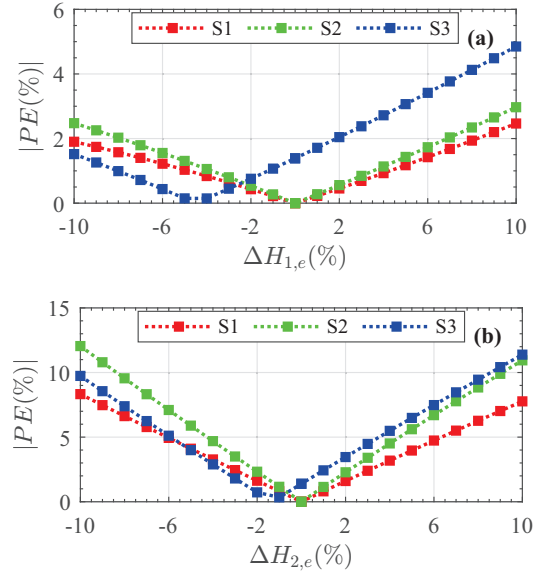


Fig. 5. Impact of linearization on the estimation of the overall inertia. *PE* for H'_{sys} when: (a) only H_1 change and (b) when only H_2 change.

PE are reported. It should be noted that *PE* tends to behave differently for $\Delta H_{1,e}$ and $\Delta H_{2,e}$ variations. Nevertheless, this is expected. Indeed, the root locus analysis of Fig. 3 verifies that modal sensitivity follows different patterns with respect to the individual inertia constants of each area.

Moreover, results indicate that the use of the full set of system modes (S1) provides the most accurate estimates. The use of only the complex system modes (S2) tends to increase *PE*, albeit not significantly. The latter remark is especially true for inertia constant variations lower than 5%. However, Scenarios S1 and S2 are rather unrealistic, since individual inertia constants of each area are generally unknown and thus eigen-analysis cannot be performed. Therefore, in this paper complex modes are determined via the MP method using system responses. As shown in Fig. 5 the use of the MP generally increases the resulting *PE*. However, for all cases, the resulting *PE* is comparable with the error of S1 and S2.

B. Impact of Approximation Order

In this subsection, the impact of the MP order on *PE* is analyzed. For this purpose, a grid search approach is employed, where the MP order is sequentially increased from $n = 5$ to $n = 9$. The former value denotes the lowest order that can be used to identify oscillatory modes of the system, while the latter is the full system order. $[H_{1,e}, H_{2,e}] = [4.5 \text{ s}, 6.5 \text{ s}]$ is used as the only known state. An unknown state is derived by altering $H_{1,e}$ by 5%. Fig. 6 presents the *PE* as a function of the approximation order, i.e., the MP model order. As shown, as the MP model order increases, *PE* decreases. This is because complex modes are identified with higher precision when higher order models are used.

C. Impact of Known States

The analysis of Section V-A demonstrates that the error introduced from the linearization is non-negligible. Therefore,

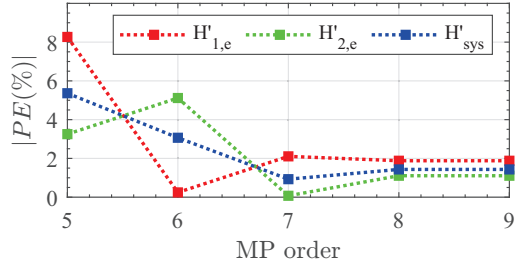


Fig. 6. Impact of MP model order on inertia estimates.

to ensure accurate inertia estimates, several known states shall be available to reduce the linearization error.

Therefore, in this Section the impact of the total number K of known states on the accuracy of the proposed method is investigated by means of a parametric analysis. In particular, five discrete cases are examined, namely C1, C2, C3, C4 and C5. In C1 only a single state is considered as available/known. In C2, C3, C4 and C5 the number of known states is two, five, ten, and twenty respectively. For these known states, $H_{1,e}$ and $H_{2,e}$ are assumed equal and uniformly distributed in the range between 3.5 s and 7.5 s. For each case, a set of 10,000 Monte Carlo (MC) simulations is performed to emulate cases with unknown inertia constants. In each MC simulation, $H'_{1,e}$ and $H'_{2,e}$ are randomly set between 3.5 s and 7.5 s and the corresponding ΔP_{tie} responses are forwarded as inputs to the MP method to identify system oscillatory modes. The *RMSD* index is used to determine for each MC the closest known state and thus the corresponding sensitivity matrix.

PE results for the estimated H'_{sys} across the examined cases are summarized in Fig. 7 by means of cumulative distribution functions (CDFs). As shown, for all examined cases a limited number of outliers is observed. To provide further insights concerning the accuracy of the methods, outliers are removed using the interquartile range rule (IQR). The resulting minimum, maximum, median values as well as the 25th (Q1) and 75th (Q3) percentiles of *PE* are presented in Table IV. As shown, as the number of known states increases, the

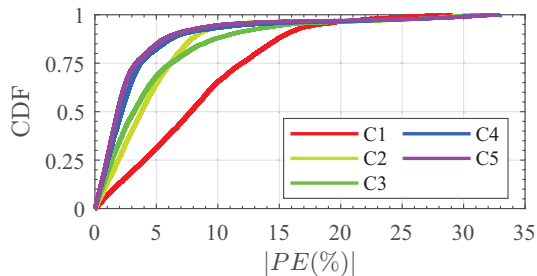


Fig. 7. *PE* for H'_{sys} by means of CDFs.

TABLE IV
STATISTICAL ANALYSIS OF *PE* VALUES ACROSS THE EXAMINED CASES

Measure	C1	C2	C3	C4	C5
Minimum	0.0015	0.0006	0.0006	0.0002	0.0001
Q1	4.0282	1.9173	1.3957	1.0572	0.9578
Median	7.8127	3.8046	3.1806	2.1851	1.8382
Q3	11.9648	6.1367	6.1934	3.6937	3.3462
Maximum	23.8698	12.4660	13.3899	7.6486	6.9287

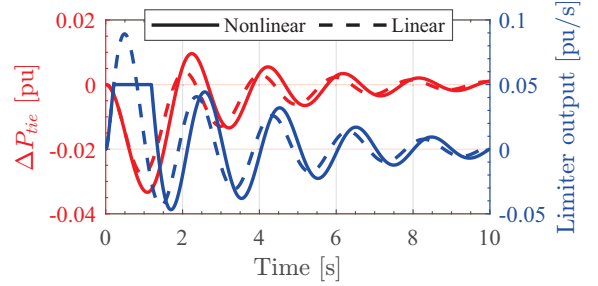


Fig. 8. Comparison of Area#1 limiter output and ΔP_{tie} responses for the linear and the nonlinear case.

performance of the proposed method is generally enhanced. Nevertheless, it is worth noting that a saturation effect is observed. Indeed, statistical indexes of Table IV reveal that the use of more than ten known states do not significantly increase the accuracy of the proposed method.

D. Impact of GRC

Here, the impact of nonlinearities, introduced by the GRC, on the accuracy of the proposed method is investigated. For this purpose, the following analysis is performed: A known system state with $[H_{1,e}, H_{2,e}] = [4.5 \text{ s}, 6.5 \text{ s}]$ is considered and the modal sensitivity matrix is computed using the linear state space representation of the examined system. An unknown state is obtained by increasing $H_{1,e}$ by 5%. For this unknown state, a sufficiently large disturbance ($\Delta P_{D1} = 5\%$) is introduced to trigger GRC nonlinearities.

In Fig. 8 Area#1 limiter output and ΔP_{tie} responses are compared for the linear case (dashed lines), where GRC is neglected, as well as for the nonlinear case (solid lines), where GRC is considered. For demonstration purposes, only the first 10 s of the responses are presented. As shown, the activation of the limiter has a significant impact on the resulting oscillations. This is especially true for the first seconds of the responses, during which the limiter is active. Nevertheless, after few seconds, the responses of the linear and the nonlinear systems practically coincide. Indeed, after few seconds nonlinearities are eliminated and only electromechanical oscillations, which are strongly related with the inertia constants, remain in the responses. Therefore, since the method is based on the modal sensitivity matrix, responses reflecting the linear part of the system shall be used for the identification of modal parameters. This can be easily achieved by forwarding to the MP method data captured a few cycles after the disturbance. In this example, MP can be applied using data obtained after $t = 4 \text{ s}$, $t = 6 \text{ s}$, and $t = 8 \text{ s}$, leading to *PE* for the overall system inertia equal to 2.16%, 1.13% and 1.50%, respectively.

VI. EVALUATION ON DIFFERENT POWER SYSTEM TOPOLOGIES

Here, the performance of the proposed method is tested on a single area power system with no external interconnections as well as on a fully interconnected three-area power system. The examined one-area system is generated by considering only Area#1 of Fig. 1. The resulting system is described by a 4th-order state-space model and contains one oscillatory mode.

The three-area power system is created by adding a third area (Area#3) in the model of Fig. 1. Area#3 is interconnected with both Area#1 and Area#2. Parameters of Area#3 are: $R_3 = 2.4 \text{ Hz/MW}$, $D_3 = 0.0083 \text{ pu/Hz}$, $T_{t3} = 0.3 \text{ s}$, $T_{g3} = 0.08 \text{ s}$, $B_3 = 0.425 \text{ MW/Hz}$, $T_{1,3} = 0.6 \text{ s}$, $T_{2,3} = 0.491 \text{ s}$ [17]. Additionally, controllers are re-tuned to enhance system stability: $P_1 = P_2 = P_3 = 0.2$, $I_1 = I_2 = I_3 = 0.5 \text{ Hz}$. The system is described by a 15th-order state space model and contains three complex conjugate modes.

A. One-Area Power System Model

To statistically evaluate the performance of the proposed method, 10,000 MC simulations are performed. For each MC only a single state is considered known, i.e., $K=1$. As discussed in Section V.C, the use of only one known state corresponds to the worst case scenario. The known state is generated by randomly setting $H_{1,e}$ in the range [3.5 s, 7.5 s]. Subsequently, an unknown state is derived by altering $H_{1,e}$ by $\pm 5\%$ and a random disturbance is introduced. $y(t) = \Delta f_1$ is recorded and used for modal identification. A 3rd order MP model is used. PE across all MCs is statistically analyzed and outliers are removed by means of IQR. The resulting average PE is 5.84%, thus verifying the accuracy of the method for the analysis of one-area power systems.

B. Three-Area Power System Model

Once again 10,000 MC simulations are conducted. Similar to Section VI-A, only one state is considered known for each MC. Known states are created by randomly setting $H_{1,e}$, $H_{2,e}$, and $H_{3,e}$ in range [3.5 s, 7.5 s]. Unknown states are derived by varying $H_{1,e}$, $H_{2,e}$, and $H_{3,e}$ by $\pm 5\%$. For each MC random disturbances are introduced and ΔP_{tie} responses are recorded and forwarded to MP. A 9th-order MP model is used for mode identification. Statistical analysis is performed for the resulting PE and outliers are removed using IQR. The mean PE is 3.42%, confirming the accuracy of the proposed method.

VII. CONCLUSIONS

In this paper, a new methodology for the inertia estimation of multi-area power systems is formulated. The proposed method uses system responses, obtained during real-time operation, to identify system modes by applying the MP method. Using the identified modes and the modal sensitivity matrix of the grid, the overall inertia level of the examined power system is estimated. The accuracy of the method is evaluated by performing simulations in one-, two-, and three-area power systems. The impact of several factors on the performance of the proposed method is quantified by means of parametric analyses and MC simulations.

Results reveal that the order of the MP model and the total number of the available known states, have a significant impact on the accuracy of the proposed method. Nevertheless, the use of more than ten known states and the approximation of the system responses using the iterative procedure of [20] can ensure accurate inertia estimates.

Further research will be conducted to test the accuracy of the proposed method under noisy conditions as well as to

investigate the performance of the method in cases where RESs are operated under virtual SGs control schemes, thus contributing to frequency support of the power system.

REFERENCES

- [1] H. Bevrani, H. Golpira, A. R. Messina, N. Hatziargyriou, F. Milano, and T. Ise, "Power system frequency control: An updated review of current solutions and new challenges," *Electr. Power Syst. Res.*, vol. 194, 2021.
- [2] ENTSO-E, "High penetration of power electronic interfaced power sources and the potential contribution of grid forming converters," Technical Report, 2019.
- [3] G. C. Kryonidis, *et. al.*, "Ancillary services in active distribution networks: A review of technological trends from operational and online analysis perspective," *Renew. Sust. Energ. Rev.*, vol. 147, 2021.
- [4] K. Prabhakar, S. K. Jain, and P. K. Padhy, "Inertia estimation in modern power system: A comprehensive review," *Electr. Power Syst. Res.*, vol. 211, 2022.
- [5] U. Tamrakar, D. A. Copp, T. Nguyen, T. M. Hansen, and R. Tonkoski, "Optimization-based fast-frequency estimation and control of low-inertia microgrids," *IEEE Trans. Energy Convers.*, vol. 36, no. 2, pp. 1459–1468, 2021.
- [6] E. Kontis, I. Pasiopoulou, D. Kirykos, T. Papadopoulos, and G. Papagiannis, "Estimation of power system inertia: A comparative assessment of measurement-based techniques," *Electric Power System Research*, vol. 196, 2021.
- [7] T. Kerdpol, M. Watanabe, R. Nishikawa, Y. Hayashi, and Y. Mitani, "Inertia estimation of the 60 Hz Japanese power system from synchrophasor measurements," *IEEE Trans. Power Syst.*, pp. 1–1, 2022.
- [8] ENTSO-E, "Future system inertia 2," Technical Report, 2018.
- [9] M. Sun, Y. Feng, P. Wall, S. Azizi, J. Yu, and V. Terzija, "On-line power system inertia calculation using wide area measurements," *Int. J. Electr. Power Energy Syst.*, vol. 109, 2019.
- [10] T. Kerdpol, M. Watanabe, Y. Mitani, and I. Ngamroo, "Inertia assessment from transient measurements: Recent perspective from Japanese wams," *IEEE ACCESS*, vol. 10, pp. 66 332–66 334, 2022.
- [11] S. C. Dimoulias, E. O. Kontis, and G. K. Papagiannis, "Inertia estimation of synchronous devices: Review of available techniques and comparative assessment of conventional measurement-based approaches," *Energies*, vol. 15, no. 20, 2022.
- [12] T. Inoue, H. Taniguchi, Y. Ikeguchi, and K. Yoshida, "Estimation of power system inertia constant and capacity of spinning-reserve support generators using measured frequency transients," *IEEE Trans. Power Syst.*, vol. 12, no. 1, pp. 136–143, 1997.
- [13] C. Phurailatpam, Z. H. Rather, B. Bahrani, and S. Doolla, "Measurement-based estimation of inertia in ac microgrids," *IEEE Trans. Sustain. Energy*, vol. 11, no. 3, pp. 1975–1984, 2020.
- [14] G. Cai, B. Wang, D. Yang, Z. Sun, and L. Wang, "Inertia estimation based on observed electromechanical oscillation response for power systems," *IEEE Trans. Power Syst.*, vol. 34, no. 6, pp. 4291–4299, 2019.
- [15] M. Crow and A. Singh, "The matrix pencil for power system modal extraction," *IEEE Trans. Power Syst.*, vol. 20, no. 1, pp. 501–502, 2005.
- [16] P. Kundur, *Power system stability and control*. New York: McGraw-Hill, 1994.
- [17] H. M. Hasanien and A. A. El-Fergany, "Symbiotic organisms search algorithm for automatic generation control of interconnected power systems including wind farms," *IET Gener. Transm. Distrib.*, vol. 11, no. 7, pp. 1692–1700, 2017.
- [18] S. Guo, S. Norris, and J. Bialek, "Adaptive parameter estimation of power system dynamic model using modal information," *IEEE Trans. Power Syst.*, vol. 29, no. 6, pp. 2854–2861, 2014.
- [19] S. Guo and J. Bialek, "Synchronous machine inertia constants updating using wide area measurements," in *2012 3rd IEEE PES Innovative Smart Grid Technologies Europe (ISGT Europe)*, 2012, pp. 1–7.
- [20] E. O. Kontis, T. Papadopoulos, G. A. Barzegkar-Ntovom, A. I. Chrysochos, and G. K. Papagiannis, "Modal analysis of active distribution networks using system identification techniques," *Int. J. Electr. Power Energy Syst.*, vol. 100, pp. 365–378, 2018.
- [21] A. Fernandez-Guillamon, A. Viguera-Rodriguez, and A. Molina-Garcia, "Analysis of Power System Inertia Estimation in High Wind Power Plant Integration Scenarios," *IET Renew. Power Gener.*, vol. 13, no. 15, pp. 2807–2816, 2019.
- [22] M. Krpan and I. Kuzle, "Introducing low-order system frequency response modelling of a future power system with high penetration of wind power plants with frequency support capabilities," *IET Renew. Power Gener.*, vol. 12, no. 13, pp. 1453–1461, 2018.